processes

MDPI

Article

Design, Development, and Performance Evaluation of a New Photovoltaic-Thermal (PVT) Air Collector: From Lab Testing to Field Measurements

Raquel Simón-Allué *, Raúl Villén, Gonzalo Brun, Yolanda Lara and Isabel Guedea

ENDEF Solar Solutions, 50820 Zaragoza, Spain
* Correspondence: raquel.simon@endef.com; Tel.: +34-976-36-58-11

Abstract: Over the last decade, the market has experienced a growing interest in hybrid photovoltaic-thermal (PVT) technologies, although more long-term studies are needed before air-based PVT panels are fully implemented. In this paper, we present the experimental framework developed around an air-based PVT collector, consisting of a high-quality photovoltaic laminate and a newly designed thermal absorber. The experimental performance of the collector was measured both in lab testing and in a pilot plant during one of the field operations. Results show an almost constant electrical performance of 15–19%, and a thermal performance that changes a lot, ranged between 15–52% for the individual panel and 11–35% for the system of 2.5 panels in series (to maximize output temperature). Field operation presents average thermal and electrical efficiencies ranged between 16–20% with an electrical–thermal generation ratio close to 1:1.

Keywords: air collectors; photovoltaic-thermal; experimental testing

check for updates

Citation: Simón-Allué, R.; Villén, R.; Brun, G.; Lara, Y.; Guedea, I. Design, Development, and Performance Evaluation of a New Photovoltaic-Thermal (PVT) Air Collector: From Lab Testing to Field Measurements. *Processes* **2023**, *11*, 588. https://doi.org/10.3390/pr11020588

Academic Editor: Blaž Likozar

Received: 9 January 2023
Revised: 9 February 2023
Accepted: 10 February 2023
Published: 15 February 2023

Copyright: © 2023 by the authors. Licensee MDPI, Basel, Switzerland. This article is an open access article distributed under the terms and conditions of the Creative Commons Attribution (CC BY) license (https://creativecommons.org/licenses/by/4.0/).

1. Introduction

Photovoltaic-thermal (PVT) panels are able to produce thermal and electrical energy simultaneously on the same module, maximizing the energy generation per solar area. This technology is gaining presence in the solar energy landscape, as pointed out by the International Energy Agency through Task 35—PV/Thermal Systems [1] and Task 60—Applications of PVT Collectors [2].

PVT panels can be classified according to the thermal exchange fluid. Although liquid-based panels (water, water + glycol, oil) present greater values of thermal performance and achieve higher temperatures, they also bring several associated drawbacks such as complex installations, higher investment costs, or more severe damage in case of leaks [3,4]. As an alternative, air-based PVT panels are being explored, with the aim of producing electricity and cheap hot air that can be used to partially supply heating, for ventilation purposes and even in non-residential applications such as food dryers.

The air circulation though the panel can be performed by natural convection or forced ventilation, for which a fan device must be installed. Natural convection avoids any electrical consumption and reduces the maintenance, but presents very low thermal efficiencies due to the decrease of the mass flow rate [5]. Its use is mainly recommended for low-moisture-content crops [6] or façade ventilation [7]. On the contrary, forced ventilation is preferred despite the electrical consumption of the fan, due to the increase of thermal performance and the possibility of using more complex geometries. Most of the results presented in literature correspond to forced ventilation.

Air-based PVT geometry is considered simpler than liquid-based PVT panels, since the sealing is recommended but is not considered as mandatory. The air path through the panel is key to determining the heat transmission, the pressure drop of the system, and the maximum flow rate. Regarding geometry, double-pass absorbers are considered to be more thermally efficient than single-pass ones, but they also bring more complexity and

a higher pressure drop. In this regard, Hegazy [8] presented a comparison between four air PVT collectors, concluding that double single-pass was the most suitable design for solar exploitation. Higher thermal efficiency values were found to rise up to 71–83% and correspond to double-pass collectors, without PV generation.

The heat transfer from the PV laminate to internal air can be enhanced through the insertion of specific obstacles in the air channel. Nadda et al. [9] analyzed the Reynolds and Nusselt numbers for different dispositions of impinging jets, concluding that for particular conditions, the thermal performance supplied by the impinging jet is up to three times superior to those formed by conventional convective cooling technologies. The use of fins and obstacles has also been explored, through numerical [10,11] and experimental approaches [12]. Fan et al. [13] presented a dynamic model validated with experimental data, helpful for determining the optimal operational conditions and design parameters (height and number of fins) of a PVT solar air heater. Hu and Zhang [14] presented an interesting review of solar air collectors based on the air flow reorganization. This study also highlights the thermal improvement due to the use of fins and jets, but also warns about the extra power consumption derived from its use.

The performance values of air PVT systems present a great divide in literature, due to the non-homogeneity of the systems encountered and the different applications. Electrical performance seems to be mainly linked to the nominal efficiency of the PV laminate, and slightly vary with the operational conditions. However, thermal performance is strongly dependent on the air flow rate, external wind speed, and air path through the panel (obstacles, fins, jets, and V-grooved design) [15]. Some experimental studies carried out in controlled conditions on PVT collectors presented very scattered thermal efficiencies: 40–65% for double-pass [16], 62–80% (depending on the fin material and frequency) for single-pass with a very high flow rate [17], up to 55% for glazed single-pass [18], or 32–48%, depending on the flow rate [19]. All the electrical efficiencies remained between 8–12%. Fewer studies are presented for systems in field operation or long-term analysis. In those cases, the thermal efficiencies are lower, with average daily values of 23.7% [20] or in the range of 20–30% depending on the season [21]. In those cases, electrical efficiencies remained below 10%.

In terms of application, recent work focuses on building-integrated photovoltaic-thermal (BIPVT) [22–24] systems for ventilation or heating supply, general drying [25], [26], greenhouse use [6,27], food drying [28–30], or multiple uses [20,31]. According to Kumar et al. [32], there is still room for improvement in the area of hybrid PVT air collectors. Other authors [15,33] highlight that despite the amount of work found in literature, the number of PVT systems at the commercial level are very limited. For that purpose, long-term studies are required.

In this work, we present the experimental performance of a new design of an air-based PVT panel, consisting of a high-performance photovoltaic laminate and a new design for a single-pass thermal absorber, whose geometry has been patented by the authors. The thermal and electrical performances have been addressed in controlled conditions (lab testing) and under real operation (one-year performance in an office building). The long-term results derived from this work help to evaluate the technical viability of this technology and the preferred configuration (parallel, series, and optimal flow) with regard to the user application.

2. Material & Methods

2.1. Prototype Description

The air-based PVT panel is composed of a 380 W mono-Si photovoltaic panel in combination with a back air chamber where air is passed through forced ventilation. The aim is a double simultaneous production: electrical energy due to the PV panel and thermal energy in form of hot air, due to the forced ventilation. The path of the air through the back of the panel is driven by a thermal absorber, where linear obstacles have been included to distribute the flow in a uniform way through the back surface and to maximize the thermal

interaction between air flow and PV cells (similar to that studied in [12,34,35]). The shape and location of these obstacles were experimentally defined. The section view of the panel is shown in Figure 1 and main features of PVT panels are included in Table 1.



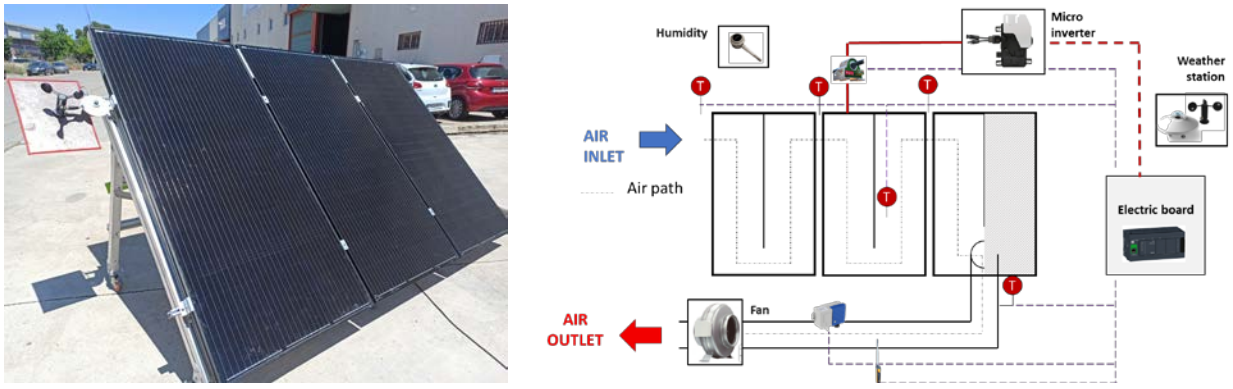
Figure 1. Section view of air-based PVT panel.

Table 1. Main features of PVT panel.

PVT Module Characteristics	Value	Units
PVT type	unglazed	-
Dimensions	1.984 × 999	mm × mm
Gross area, A_G	1.98	m^2
N° cells/PV cell type	72/mono-Si	-
Nominal power (STC)	380	W
Nominal efficiency (STC)	19.0	%
Voltage at MPP, V_{mppt}	40.26	V
Current at MPP, I_{mppt}	9.44	A
Temperature coefficient of power	−0.39	%/°C

2.2. Lab Testing

The experimental testing rig of the prototypes was constructed following the indications of the standard ISO 9806:2017—Solar energy. Solar thermal collectors. Test methods [36]. The testing bench was designed for three panels, in order to be able to evaluate not only the performance of one isolated panel but also the combination of two or three in a row, to obtain higher output temperatures. The scheme of the final setup is shown in Figure 2.



(**a**) (**b**)

Figure 2. Testing bench of air-based PVT panels: (**a**) Frontal view of real set-up; (**b**) Scheme of set-up with main equipment and sensors.

The inclination of the structure was fixed to 45 °C, based on the latitude of the testing location (Zaragoza). Tests were carried out during the months of summer and winter under natural irradiance. Testing rig was manually oriented to the sun during central solar hours of the day in order to guarantee a solar irradiance between 850–1000 W/m^2. Solar radiation and wind speed were measured in the collector plane.

The hydraulic connection is performed so that the heat exchange fluid (air) flows in an open loop, crossing all panels on its way. The air is moved by forced ventilation with the

fan (model: CK 200 B, 145 W nominal power) located at the outlet of the panels, working in suction mode. Electrical production of the PVT prototype is generated in DC power and turned into AC power through the micro inverter located on the back side of the panel. The micro inverter model integrated in each panel of the testing rig is an ENPHASE IQ 7+.

Following the requirements of the ISO 9806:2017, a list of measurement sensors and monitoring devices were installed on strategic points of the testing rig in order to obtain useful and reliable data for the analysis. The measured magnitudes were air temperature (inlet and outlet of each panel), cell temperature in the middle panel, pressure drops in the system, volumetric flow, and DC current generated in the panels. The position of the sensors is shown in Figure 2. The testing rig also includes a weather station (composed by pyranometer, anemometer, and humidity meter) to measure the environmental conditions. The data were continuously monitored in a PLC Modicon 241 and computationally registered for the postprocessing. The description of the main measurement instruments is included in Table 2.

Table 2. Technical description of the main measurement instruments.

Magnitude	Sensor Model	Amount	Range	Accuracy
Temperature	Pt100, several brands	10	−50–400 °C	±0.05 °C
Pressure	Gems, 526610CLBACT1C-RS	1	±1000 Pa	±1%
Volumetric flow	Testo 405i	1	0–30 m/s	0.3 m/s ± 5 vm%
Wind speed	Darrera, SKU: 3R FWS	1	0.5–50 m/s	±0.1 m/s
Rel. Humidity	SEM160i RH	1	0 to 100%RH	±3%
Irradiance	Pyranometer, LP PYRA 03 AC	1	0–2000 W/m^2	0.025 W/m^2
Current	HT-RS-0, Herten SL	2	0–10 V	±0.5%
Voltage	In-home sensor	1	-	-

2.3. Pilot Plant Description

The real performance of this panel has been analyzed through one-year operation in a real environment. The pilot plant is located on the roof of an industrial company in Zaragoza (Spain), to provide electricity and contribute to thermal supply for an office. The solar plant is composed of a bench of 5 PVT panels in a row, forming two individual hydraulic circuits that merge on the central panel (see Figure 3). Panels were placed facing south, with a deviation of 5° west, and a tilt of 45° to maximize thermal production in winter. The resulting bench has two inlets (on the sides) and only one outlet (on the central panel). As a result, the pilot plant reproduces the scheme of the testing rig, with two circuits in parallel.



Figure 3. 5-panel PVT pilot plant on industrial facility.

The air extracted from the panels is led into the building with a double-walled duct with glass-fiber insulation. Ventilation is forced by means of a centrifugal fan CK 200 B, same model as that used in Section 2.2 *Lab testing*. Depending on the inner office temperature, hot air is headed directly into the office (heating mode) or released back into the environment (dissipation mode), through the actuation of dumping gates.

Thermal control of the installation is performed through the RESOL control unit DeltaSol® CS/4. This units regulates both the operation of the fan (only ON–OFF modes) and the dumping gates. The control is executed based on the system temperatures and heating requirements in the office.

From the electrical point of view, panels in the field are electrically connected in series and connected to one of the MPPT trackers of the inverter SUN2000L-3KTL (Huawei). Electrical power installed raises to 1.9 kWp.

2.4. Measure of Uncertainty

The analysis of the uncertainty in the field performance has been calculated based on the accuracy and resolution values of the monitoring devices listed in Table 2. For each magnitude, the relative and absolute error have been calculated and shown in Table 3. As can be seen in this table, the main source of error is the flow measurement, which involves the difficulty of measuring a fluid in motion inside a pipe. This uncertainty is transferred to the measurement of thermal power and efficiency, making their uncertainty rise to 9.5%. In the rest of the cases, the relative error does not exceed 1%.

Table 3. Values of absolute and relative error for main magnitudes in testing rig.

Magnitude	Unit	Absolute Error	xi	Relative Error
Temperature gap	°C	0.100	30	0.33%
Volumetric flow	m^3/h	13.52	150	9.01%
Solar Irradiance	W/m^2	1.000	800	0.13%
Thermal power	W	28	300	9.35%
Thermal efficiency	%	0.024	0.25	9.47%
Electrical power	W	2	280	0.66%
Electrical efficiency	%	0.001	0.177	0.79%

2.5. Mathematical Considerations

The evaluation of the thermal and electrical performance of the prototype was addressed following the indications of ISO 9806:2017, based on the information acquired by the different sensors and measuring equipment installed in the testing rig and the pilot plant.

In order to obtain the thermal performance of each prototype, it is necessary to previously calculate the mass flow rate ($\dot{m}M$), which can be obtained from the volumetric flow rate ($\dot{m}V$) and the fluid density. The density has been estimated considering the air temperature, ambient pressure, and the air humidity content when this data was available.

Thus, the mass flow rate is calculated as:

$$\dot{m}M = \dot{m}V \times \rho_{air} \quad (1)$$

The instantaneous effective power generated by each prototype is calculated as in Equation (2), where $\dot{m}M$ is the mass flow rate of the fluid in the rig, c_f corresponds to the specific heat of air, and ΔT to the thermal gap of the fluid in one panel of the whole system (between the inlet of Panel 1 and the outlet of Panel 3). Based on this effective power, the instant thermal efficiency of the prototype is defined as in Equation (3), with A_G being the gross area of the photovoltaic surface and G the amount of solar irradiance measured in-plane by the pyranometer in W/m^2.

$$\dot{Q} = \dot{m}M \cdot c_f \cdot \Delta T \quad (2)$$

$$\eta_{th} = \dot{Q}/(A_G \cdot G) \quad (3)$$

The electrical performance of the PVT prototypes was evaluated by calculating the electrical power and PV efficiency. In the testing rig, the electrical output is calculated through the current value measured by the current isolator HT-RS-0 and a voltage divider installed at the output of the intermediate panel. In the pilot plant, both magnitudes were directly registered by the solar inverter.

In both cases, electrical power W_p is calculated from the current (I) and voltage (V) as indicated in Equation (4) and PV efficiency through Equation (5).

$$W_p = I \cdot V \quad (4)$$

$$\eta_{PV} = W_p/(A_G \cdot G) \quad (5)$$

3. Results & Discussion

3.1. Determination of Relevant Operational Parameters

To determine the main external parameters influencing the operation of air-based PVT panels, we have carried out a multiple linear regression analysis to assess their significance on the thermal and electrical efficiency (η_{PV}). For thermal efficiency, we have studied the results on the individual panel (η_{th}_Panel) and the whole testing bench considering 2.5 panels in series (η_{th}_Bench). The operational variables are: environmental temperature (T_a, °C), wind speed (W_{SP}, m/s), amount of fluid flow ($\dot{m}V$), and average temperature of the fluid during the operation (T_m, °C). The main statistics of the regression are also calculated to assess the robustness of the analysis. All results are shown in Table 4.

Table 4. Results of multiple linear regression analysis: Significance F (Sign. F), adjusted R square (Adj. R^2), and Standard error (SE) and linear coefficients of the independent variables.

	Sign. F	Adj. R2	SE	I0	Ta	W_{SP}	$\dot{m}V$	Tm
η_{th}_Panel	0.9387	0.9385	0.0174	−0.36468	−0.04705	−0.00157	0.00304	0.04658
η_{th}_Bench	0.9615	0.9615	0.0101	−0.15990	−0.01697	−0.00321	0.00179	0.01605
η_{PV}	0.5320	0.5309	0.0042	0.21489	−0.00028	−0.00056	0.00000	−0.00083

Results indicate (with a p-value < 0.05) that all operational variables proposed are significant for each of the thermal and electrical efficiencies studied. It means that they are relevant to the study as they have an effect on the final value. As a general rule, an increase on the operational temperature and amount of fluid flow has a positive effect on the thermal efficiency, but a negative effect on the electrical one. On the other hand, an increase on environmental temperature or wind speed seems to affect both electrical and thermal performance negatively.

3.2. Lab Testing

The testing bench configuration, with 2.5 panels connected in series, allowed us to evaluate not only the individual panel but also the whole system, as it is planned to be installed in future installations where higher temperature gap is needed. The testing showed a higher thermal efficiency for the first panel rather than the following. Thermal efficiency ranged between 19–52% for the first panel and 11–35% for the whole testing system (2.5 panels), depending on the operating conditions. The electrical production showed a more constant behavior with less influence from the operating conditions, with efficiency values ranged between 15–19%.

The most influential parameter during the tests was the air flow, which agrees to that reported by many authors [15,37,38]. In the testing, the air flow rate was varied from 62.5 to 162.5 m^3/h. The thermal and electrical efficiencies registered during the testing are shown in Figure 4, as well as the trend lines. The first panel showed higher thermal efficiency values than the whole system, and a positive relation with the increase of the flow rate. The

thermal performance of the first panel rose around 2.26% with each 10 m^3/h increment of air between 20–40 °C. The electrical efficiency remained almost constant.

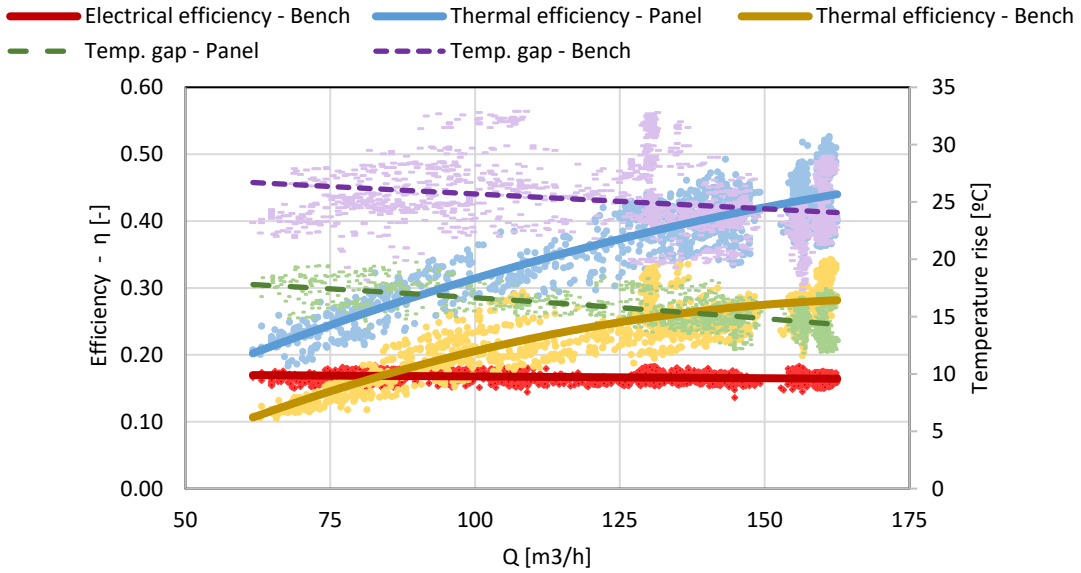


Figure 4. Variation of instant efficiency of individual panel, testing bench, and temperature rise versus air fluid flow inside the panel.

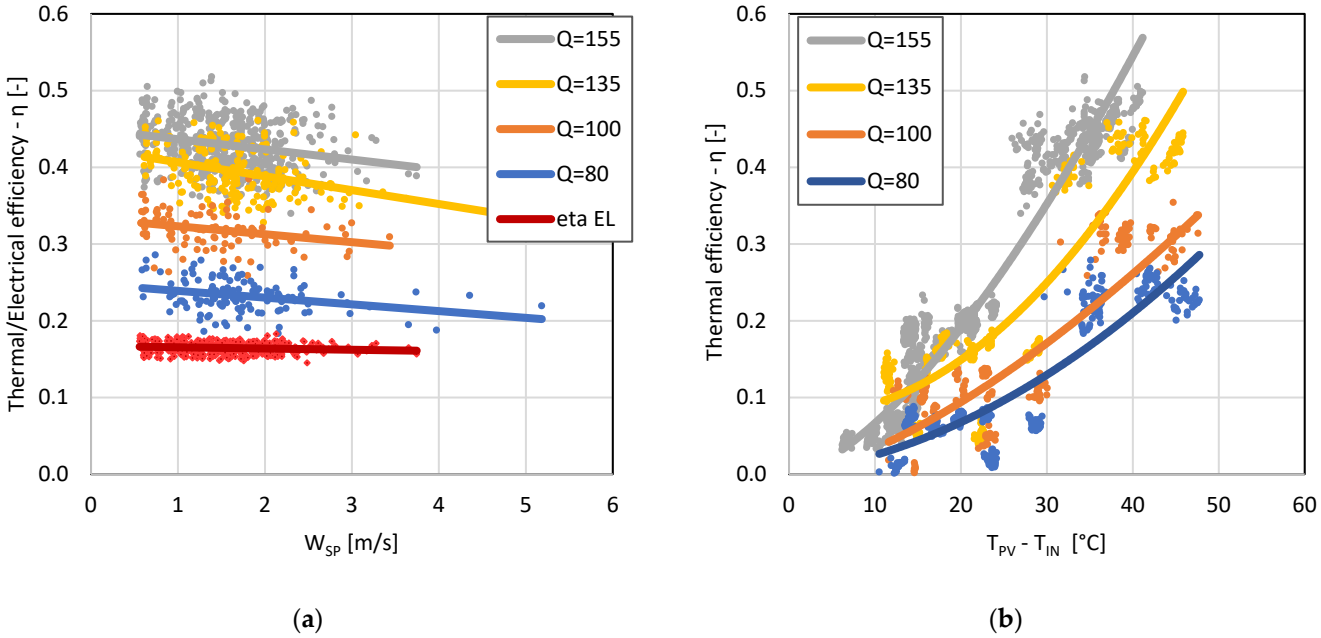
These thermal performance values are in line with others found in literature for similar configuration of air/PVT panels, i.e., average values of 36.26% for 0.022–0.060 kg/s (approx. 68–186 m^3/h) flow rate range reported by Huang et al. [39] and 35–45% for 223 m^3/h reported by Amori et al. for single duct single pass [16]. It should be remarked that both of them present electrical efficiencies below 10%, which suggests that the overall efficiency of the air/PVT panel remains lower than the one presented in this article. The obtained thermal efficiencies are also slightly higher than other values found in literature, such as 27% for single-inlet [40] or 23% [41], both of which are measured experimentally at a higher operating fluid flow and electrical efficiencies between 10–15%.

Compared to water/PVT panels, air thermal performance is similar to the optical coefficient values found for some unglazed PVT panels [42,43] for a mass flow close to 0.03 kg/s. However, it should be remarked that the different nature of the fluid (water and air) makes it very difficult to compare the performance of the two types of panels. Water/PVT panels are strongly influenced by the heat losses when they operate above the environment temperature (denoted by the heat loss coefficients), while open-loop air panels operate by taking the inlet temperature of the environment, so this relation remains different. In addition, air PVT panels present a high dependency with the mass flow rate, which water PVT reflects with a much less intensity. In both cases, the use of a glazed cover could help to increase the thermal performance, by penalizing at the same time the electrical operation.

As stated before, the fluid flow rate has a strong influence on the values obtained. In order to evaluate the influence of the other variables, those have been assessed by defining similar flow rate groups. To that end, we have grouped the efficiency values of the first panel for flows around 80, 100, 135, and 155 m^3/h. Electrical results are shown all together, due to the lower influence.

Wind speed (Figure 5a) proved to have a negative effect on the thermal efficiency of the individual panel, as expected for an unglazed configuration [44,45]. This penalty seems to have a similar intensity with the independency of the flow rate, reaching a 1% decrease of absolute thermal efficiency with each m/s of wind speed increase. This assumption is however generic, since the non-uniformity of the external wind (gusts)

and the fact that there is co-dependency with other operational variables prevent a more accurate measurement.



(**a**) (**b**)

Figure 5. Thermal and electrical efficiency of individual panel grouped at different fluid flow levels (Q in m^3/h) versus: (**a**) external wind speed and (**b**) maximum temperature gain (T_{PV}–T_{IN}).

Thermal efficiency was also analyzed regarding the average temperature of the fluid during the operation (T_m) and the environmental temperature (T_a). In these cases, both variables seemed to have a very slight effect on the thermal performance with no clear trend. Instead, the effect of the fluid temperature is studied with regard to the PV laminate temperature, since it limits the maximum gain of the air through the panel. Trends are shown in Figure 5b for the studied flow rates. Attending to this figure, the temperature difference between the air in the inlet and back PV laminate proves to be key in the thermal performance of the panel, showing a strong positive influence with the increase of the temperature gap.

Results indicate that the thermal efficiency values obtained for a temperature difference of 20 °C doubled when the temperature difference rises to 32 °C, and tripled when it reaches 40 °C. This influence directly affects the type of installation of several panels in series, as it is the case with the testing bench, where the first panel maintains an acceptable efficiency but the second and third panels reduce their contribution considerably. This effect occurs regardless of the fluid rate. As a consequence, the overall efficiency of the testing bench is almost halved compared to the first panel, as it was shown in Figure 4.

As seen in Figure 4, the air flow rate inside the panel directly conditions the thermal performance of the individual panel and the full system. Although the thermal efficiency and production are enhanced with the flow rate (around 2.26% with each increase of 10 m^3/h of air between 20–40 °C), the air temperature at the outlet is reduced, and also the use that can be made of this air. To obtain higher temperatures at the output, the number of panels in series can be increased, with a consequent loss of overall efficiency, as discussed above. The optimum configuration between temperature and efficiency will depend on the use and application of the particular solar installation.

For drying purposes, for example, the temperature requirements at different seasons along the year are flexible [26,28]. Thus, the use of one or more panels in series can be selected depending on the required drying temperature or the season and location of the product. For building purposes, however, the heat generated is mainly used in winter to supply heating or ventilation, so reaching higher output temperatures is mandatory [22,46].

With the aim of maximizing the useful energy of the system, the configuration of 2.5 panels in series has been chosen for the pilot plant in an office building.

3.3. Field Measurement

3.3.1. General Performance on Annual Basis

The PVT pilot plant is performed during a complete year to supply heat and electricity to an office. The installation runs with an almost constant fluid flow of 185 m^3/h, which means 92.5 m^3/h per line. Monthly results in terms of energy generation and efficiencies are shown in Figure 6 with the environmental conditions shown in Figure 7.

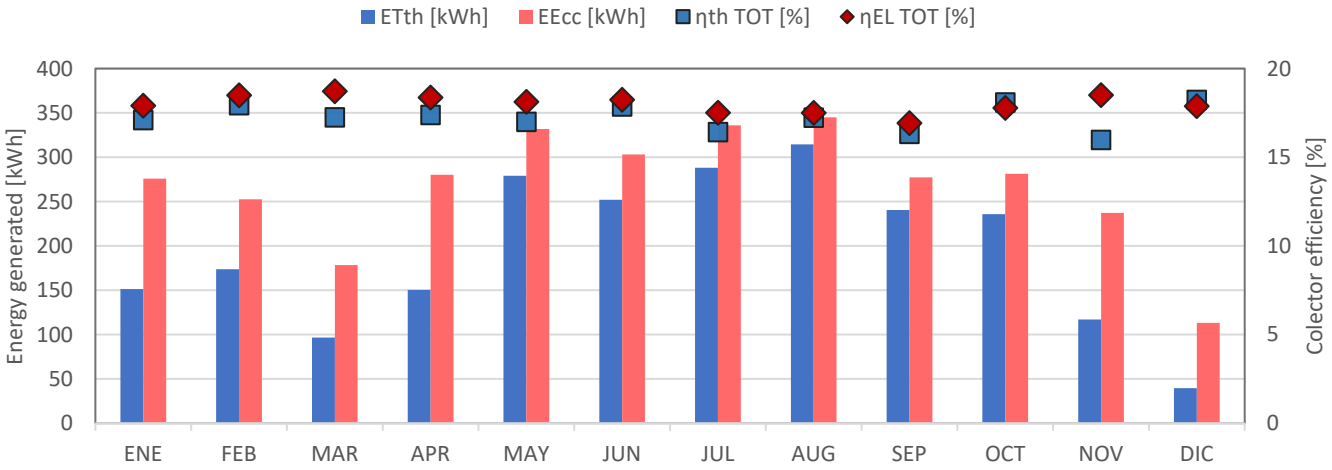


Figure 6. Monthly distribution of energy production and average efficiencies.

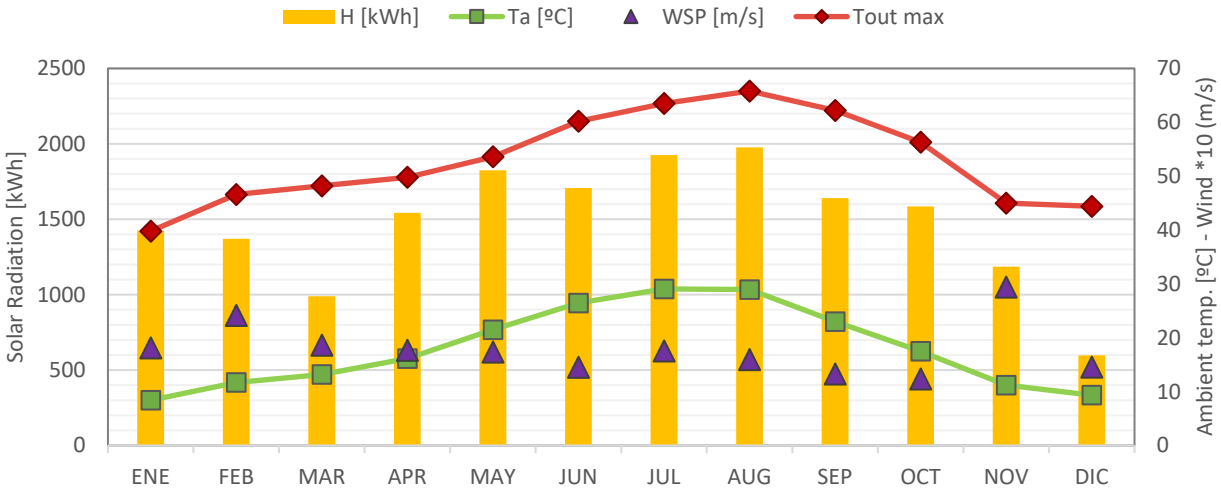


Figure 7. Average environmental conditions on year under study. Average values for ambient temperature and wind speed are calculated only during the day.

Considering the one-year operation, thermal and electrical efficiencies ranged between 16–20% with slight differences between seasons. The ratio between the thermal and electrical efficiency was close to 1, with a small decrease for months with high wind levels. These values are close to others measured in field operation, such as 23.7% [20] or 20–30% [21], both with electrical performances below 10%.

Energy production showed a great difference depending on the season, due to the strong relation to the solar resource. Electrical production showed a generation profile very similar to solar radiation, with maximum and minimum values in August (345 kWh) and December (113 kWh), respectively. Thermal production, on the other hand, depends not

only on the solar radiation but also on the fan operation. In heating mode (October to April), the fan is activated only when the solar field can contribute to the heating, that is, when heat is produced over 30 °C. In dissipation mode (May to September), the fan is activated when the system is able to produce heat, which means when heat is produced over the ambient temperature. As a result, the fan operates during more hours. Consequently, the difference between summer and winter thermal energy production is higher, with extreme values again in August (315 kWh) and December (40 kWh).

Attending to these figures, it remains clear that the application of the PVT system for supplying heating to an office limits the amount of energy generated during the winter months (October to April), since it is forced to operate above the internal office temperature to provide heat. This fact indicates that other applications are more recommended to maximize the thermal energy production and use of the installation. The most widespread application is solar dryers, as has been addressed by previous works [28,30,47] but BIPVTs are gaining relevance in the last years [32,48,49], more so in the field of Passivhaus. In this regard, we consider that the use of this air-based PVT in unheated spaces (industrial facilities and transit areas) or as a ventilation preheater in Passivhaus would allow us to make further use of the energy generation without a temperature limit.

3.3.2. Analysis of Specific Days

To better understand how the system performs in detail, we have analyzed typical operation days for winter and summer.

Figure 8 shows the detailed operation of a cloudy day (first), clear day with low wind level (second), and clear windy day (third). Figure 9 shows the instant energy and efficiency data for these particular days. On a cloudy winter day, the PV laminate is able to generate electricity during almost the whole period with sun radiation, following the irregular profile of the sun irradiance. The thermal part, however, is only activated when the PVT outlet temperature exceeds the inner temperature in the building, which in winter cloudy days is scarce. As a general rule, it has been observed that the fan is only activated when the solar radiation is above 500–550 W/m^2.

During sunny days, the perspective is very different. The period of electrical generation is still longer than the thermal operation, but remains much more similar. The thermal and electrical efficiencies along the day keep quite constant around 17–19%. The expected output temperature during peak sun hours on sunny days is in the range of 30–38 °C. At the end of the day when the ambient temperature and solar irradiance decrease, the electrical performance slightly increases due to the reduction of cell temperature, while the thermal contribution decreases. On a windy day, the wind removes the heat from the frontal face of the panel and the thermal side of the installation is strongly penalized. As a consequence, the fan starts to operate later (so the daily energy produced is lower); the thermal efficiency changes from 17.5 to 13.5% and the outlet temperature decreases a maximum of 10 degrees.

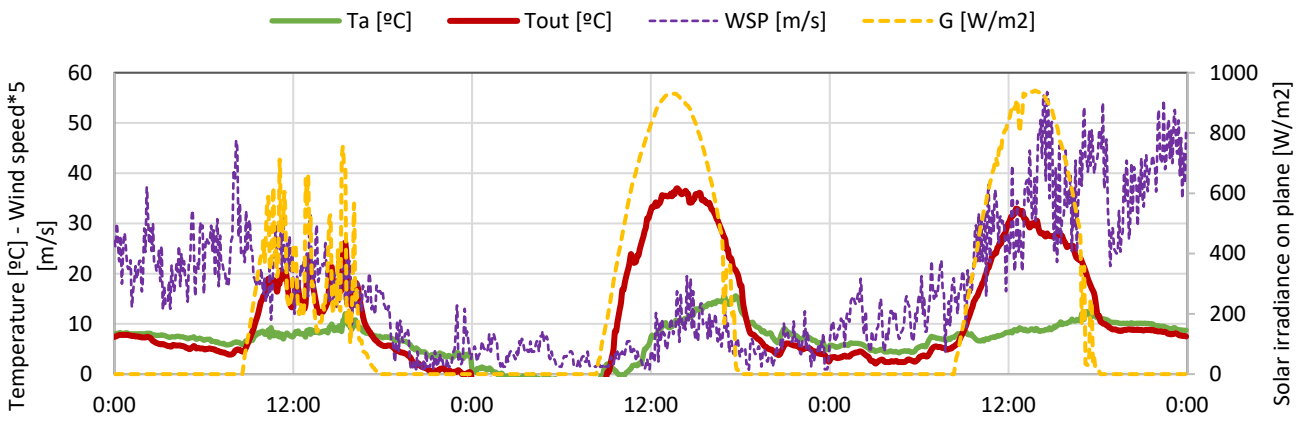


Figure 8. Detail of three days in winter: inlet/outlet temperatures, wind speed and solar irradiance.

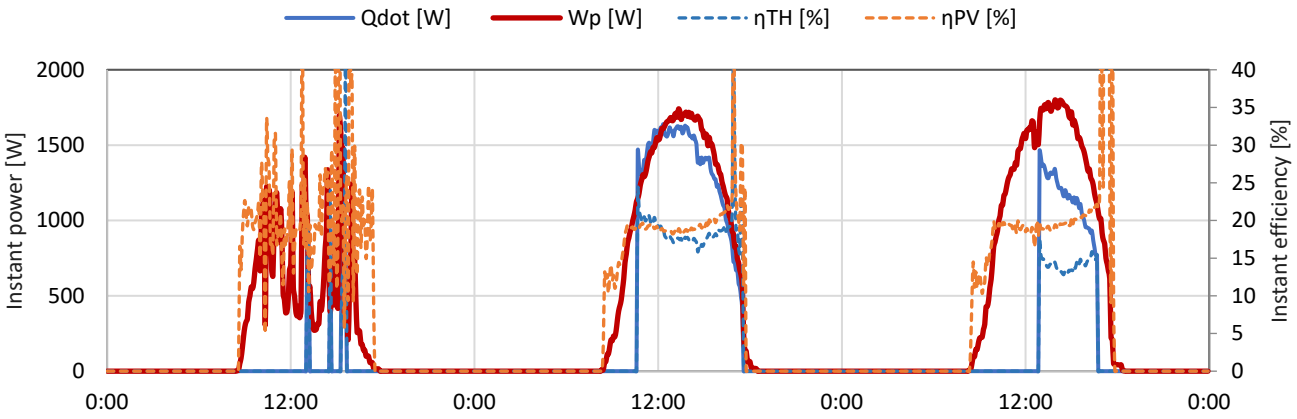


Figure 9. Detail of three days in winter: thermal and electrical power and efficiencies for a cloudy, clear, and windy day.

The detailed field operation during summer days is shown in Figures 10 and 11, again for a cloudy day (first), clear day with low wind level (second), and clear windy day (third). As a general rule, the thermal and electrical efficiencies along the day remain similar in the range of 16–18%, slightly lower than in winter. In this case, the hours with sunshine are longer than winter ones (as expected) and the level of solar radiation from which the thermal component is activated is in the range of 350–400 W/m^2.

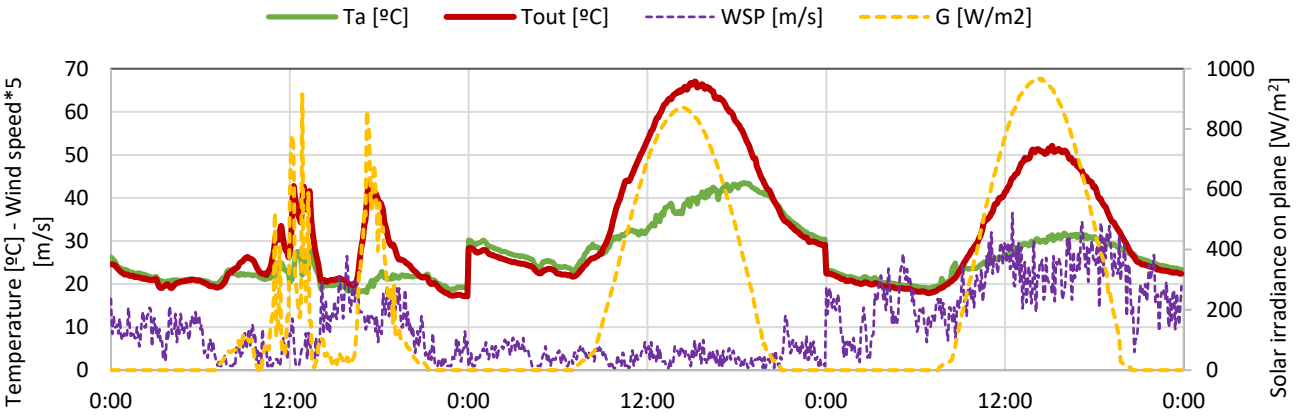


Figure 10. Detail of three days in summer: inlet/outlet temperatures, wind speed, and solar irradiance.

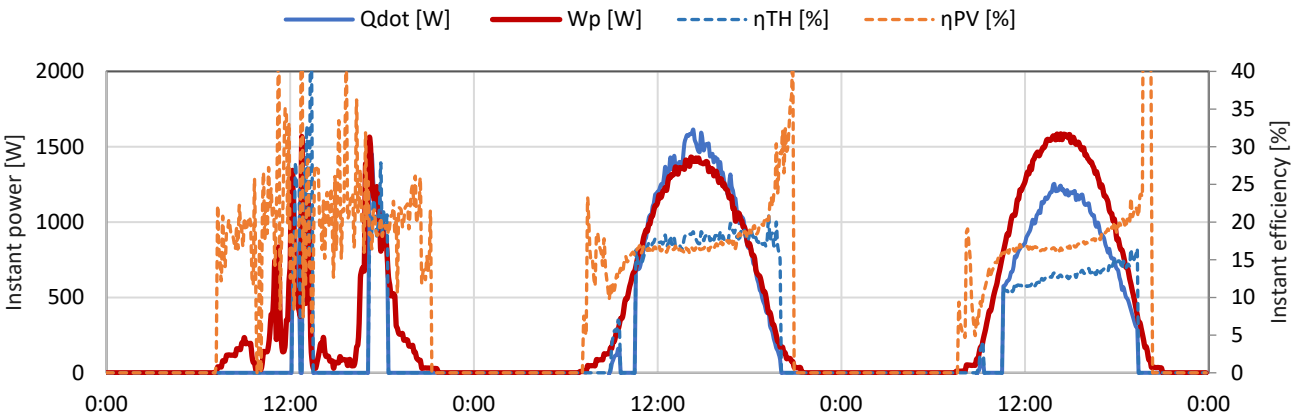


Figure 11. Detail of three days in summer: thermal and electrical power and efficiencies for a cloudy, clear, and windy day.

During a cloudy day, the system operates in a similar way as in winter: photovoltaic generation follows the irregular profile of the solar irradiation and the thermal part is only activated in small periods when the solar radiation exceeds 400 W/m^2. During a clear day, the effect of the wind on the collectors seems to be less influential than during the winter, due to the excess of heat during summer in Spain. Again, the wind provokes an increase on the photovoltaic generation but a slight decrease on the thermal performance. The most noticeable effect seems to be in the reduction of temperatures, both at the inlet and outlet of the collectors.

4. Conclusions & Future Lines

In this article, we present the performance of an air/PVT solar collector, consisting of a high-performance photovoltaic laminate and a new design of thermal absorber geometry, patented by the authors. The experimental performance has been evaluated in controlled environment (lab testing) and real operation (pilot plant) to provide heat to an office. For the lab testing, we have analyzed the thermal performance of one individual panel and 2.5 panels connected in series, in order to maximize the output temperature of the system. In the pilot plant, a five-panel bench has been installed, merging two parallel thermal circuits of 2.5 panels.

The main conclusions of the performance analysis are as follows:

- The analysis of the operation in controlled conditions showed an almost constant electrical performance, ranged between 15–19%, and a thermal performance that changes a lot, ranged between 15–52% for the individual panel and 11–35% for the 2.5-panel system.
- The thermal side proved to be highly dependent on the operational parameters of the installation, mainly on the internal flow rate and the temperature gap between the inlet and the back PV laminate, and to a lesser extent on the external wind speed. A minimum difference of 25 °C between the air inlet and PV temperature seems to be determinant for an acceptable thermal performance.
- For the individual panel, the thermal/electrical performance ratio of 1:1 is obtained at 50 m^3/h and 2:1 at 100 m^3/h. For the configuration of 2.5 panels, the thermal/electrical performance ratio of 1:1 is obtained at 80 m^3/h and 1.5:1 at 125 m^3/h.
- Regarding the pilot plant and considering the one-year operation, thermal and electrical efficiencies ranged between 16–20% (fluid flow around 92.5 m^3/h) with no significant differences between the seasons. The energy production was higher during the summer months due to the increase in the solar resource, with a more pronounced difference in the thermal rather than electrical side.
- The current configuration of 2.5 panels penalizes the thermal efficiency with regard to the individual panel, but increases the output temperature of the installation, a key factor for maximizing the energy use. Thus, the selection of several panels in series should be further analyzed according to the particular application.

The full year of operation of the plant has demonstrated that this system can work robustly, with very little maintenance, to provide electrical and thermal energy to an office. The next steps will be aimed at devising other panel layouts in a way that maximizes the energy generated at a useful temperature, without penalizing the efficiency of the system as much. Other applications besides supplying building heating should be analyzed in order to maximize the exploitation of the generated thermal energy.

5. Patents

The panel design presented in this work is protected under the EP 3 809 591 A1.

Author Contributions: Conceptualization, I.G., G.B. and R.S.-A.; methodology, R.S.-A., G.B. and R.V.; validation, R.S.-A.; formal analysis, R.S.-A.; investigation, R.S.-A. and R.V.; resources, G.B. and I.G.; data curation, R.S.-A.; writing—original draft preparation, R.S.-A.; writing—review and editing, R.S.-A., Y.L. and I.G.; visualization, R.S.-A. and Y.L.; supervision, I.G.; project administration, R.S.-A.; funding acquisition, I.G. All authors have read and agreed to the published version of the manuscript.

Funding: This project has received funding from the EuroStars-2 joint programme with co-funding from the European Union Horizon 2020 research and innovation programme, under the project PV-SolAir E!113591.

Data Availability Statement: Data is not open to general public due to privacy restrictions.

Conflicts of Interest: The authors declare no conflict of interest. The funders had no role in the design of the study; in the collection, analyses, or interpretation of data; in the writing of the manuscript; or in the decision to publish the results.

Nomenclature

AC	Alternating current
Adj. R^2	Adjusted R square
A_{PV}	Aperture area [m^2]
BIPVT	Building-integrated photovoltaic-thermal
c_f	Specific heat of air [J/Kg K]
DC	Direct current
EE_{cc}	Electrical energy in DC [kWh]
ET_{th}	Thermal energy [kWh]
G	Solar irradiance on PVT plane [W/m^2]
H	Solar radiation on PVT plane
I	Current [A]
I_{mppt}	Current circulating through the panel at maximum production stage [A]
$\dot{m}M$	Mass flow rate [Kg/s]
$\dot{m}V$	Volumetric flow rate [m^3/s]
$\dot{Q}$, *Qdot*	Thermal power [W]
PV	Photovoltaic
PVT	Photovoltaic-Thermal
SE	Standard error of regression
STC	Standard Test Conditions
T_a	Environmental temperature [°C]
T_{IN}	Inlet air temperature in a panel [°C]
T_m	Average fluid temperature inside the panel [°C]
T_{PV}	PV laminate temperature [°C]
T_{OUT}	Outlet air temperature in a panel [°C]
V	Voltage [V]
V_{mppt}	Voltage circulating through the panel at maximum production stage [V]
W_p	Electrical power [W]
W_{SP}	Average wind speed [m/s]
η_{th}	Thermal efficiency [-]
η_{PV}	Electrical efficiency [-]
α_{PV}	Voltage temperature coefficient [%/°C]
ρ_{air}	Air density [kg/m^3]
ΔT	Temperature gap between inlet and outlet of the panel [K]

References

1. IEA-SHC. Task 35—PV/Thermal Solar Systems. Available online: https://task35.iea-shc.org/ (accessed on 14 February 2022).
2. IEA-SHC. Task 60—PVT Systems: Application of PVT Collectors. Available online: https://task60.iea-shc.org/ (accessed on 14 February 2022).
3. Herez, A.; El Hage, H.; Lemenand, T.; Ramadan, M.; Khaled, M. Review on Photovoltaic/Thermal Hybrid Solar Collectors: Classifications, Applications and New Systems. *Sol. Energy* **2020**, *207*, 1321–1347. [CrossRef]

4. Besheer, A.H.; Smyth, M.; Zacharopoulos, A.; Mondol, J.; Pugsley, A. Review on Recent Approaches for Hybrid PV/T Solar Technology. *Int. J. Energy Res.* **2016**, *40*, 2038–2053. [CrossRef]
5. Shahsavar, A.; Ameri, M. Experimental Investigation and Modeling of a Direct-Coupled PV/T Air Collector. *Sol. Energy* **2010**, *84*, 1938–1958. [CrossRef]
6. Prakash, O.; Kumar, A. Solar Greenhouse Drying: A Review. *Renew. Sustain. Energy Rev.* **2014**, *29*, 905–910. [CrossRef]
7. Assoa, Y.B.; Sauzedde, F.; Boillot, B.; Boddaert, S. Development of a Building Integrated Solar Photovoltaic/Thermal Hybrid Drying System. *Energy* **2017**, *128*, 755–767. [CrossRef]
8. Hegazy, A.A. Comparative Study of the Performances of Four Photovoltaic/Thermal Solar Air Collectors. *Energy Convers. Manag.* **2000**, *41*, 861–881. [CrossRef]
9. Nadda, R.; Kumar, A.; Maithani, R. Efficiency Improvement of Solar Photovoltaic/Solar Air Collectors by Using Impingement Jets: A Review. *Renew. Sustain. Energy Rev.* **2018**, *93*, 331–353. [CrossRef]
10. Jha, A.; Tripathy, P.P. Optimization of Process Parameters and Numerical Modeling of Heat and Mass Transfer during Simulated Solar Drying of Paddy. *Comput. Electron. Agric.* **2021**, *187*, 106215. [CrossRef]
11. Fan, W.; Kokogiannakis, G.; Ma, Z. A Multi-Objective Design Optimisation Strategy for Hybrid Photovoltaic Thermal Collector (PVT)-Solar Air Heater (SAH) Systems with Fins. *Sol. Energy* **2018**, *163*, 315–328. [CrossRef]
12. Abene, A.; Dubois, V.; Le Ray, M.; Ouagued, A. Study of a Solar Air Flat Plate Collector: Use of Obstacles and Application for the Drying of Grape. *J. Food Eng.* **2004**, *65*, 15–22. [CrossRef]
13. Fan, W.; Kokogiannakis, G.; Ma, Z.; Cooper, P. Development of a Dynamic Model for a Hybrid Photovoltaic Thermal Collector—Solar Air Heater with Fins. *Renew. Energy* **2017**, *101*, 816–834. [CrossRef]
14. Hu, J.; Zhang, G. Performance Improvement of Solar Air Collector Based on Airflow Reorganization: A Review. *Appl. Therm. Eng.* **2019**, *155*, 592–611. [CrossRef]
15. Chaibi, Y.; El Rhafiki, T.; Simón-Allué, R.; Guedea, I.; Luaces, S.C.; Gajate, O.C.; Kousksou, T.; Zeraouli, Y. Air-Based Hybrid Photovoltaic/Thermal Systems: A Review. *J. Clean. Prod.* **2021**, *295*, 126211. [CrossRef]
16. Amori, K.E.; Abd-AlRaheem, M.A. Field Study of Various Air Based Photovoltaic/Thermal Hybrid Solar Collectors. *Renew. Energy* **2014**, *63*, 402–414. [CrossRef]
17. Özakın, A.N.; Kaya, F. Experimental Thermodynamic Analysis of Air-Based PVT System Using Fins in Different Materials: Optimization of Control Parameters by Taguchi Method and ANOVA. *Sol. Energy* **2020**, *197*, 199–211. [CrossRef]
18. Kong, D.; Wang, Y.; Li, M.; Keovisar, V.; Huang, M.; Yu, Q. Experimental Study of Solar Photovoltaic/Thermal (PV/T) Air Collector Drying Performance. *Sol. Energy* **2020**, *208*, 978–989. [CrossRef]
19. Saygin, H.; Nowzari, R.; Mirzaei, N.; Aldabbagh, L.B.Y. Performance Evaluation of a Modified PV/T Solar Collector: A Case Study in Design and Analysis of Experiment. *Sol. Energy* **2017**, *141*, 210–221. [CrossRef]
20. Lamrani, B.; Draoui, A.; Kuznik, F. Thermal Performance and Environmental Assessment of a Hybrid Solar-Electrical Wood Dryer Integrated with Photovoltaic/Thermal Air Collector and Heat Recovery System. *Sol. Energy* **2021**, *221*, 60–74. [CrossRef]
21. Aste, N.; Chiesa, G.; Verri, F. Design, Development and Performance Monitoring of a Photovoltaic-Thermal (PVT) Air Collector. *Renew. Energy* **2008**, *33*, 914–927. [CrossRef]
22. Maghrabie, H.M.; Elsaid, K.; Sayed, E.T.; Abdelkareem, M.A.; Wilberforce, T.; Olabi, A.G. Building-Integrated Photovoltaic/Thermal (BIPVT) Systems: Applications and Challenges. *Sustain. Energy Technol. Assess.* **2021**, *45*, 101151. [CrossRef]
23. Abdelrazik, A.S.; Shboul, B.; Elwardany, M.; Zohny, R.N.; Osama, A. The Recent Advancements in the Building Integrated Photovoltaic/Thermal (BIPV/T) Systems: An Updated Review. *Renew. Sustain. Energy Rev.* **2022**, *170*, 112988. [CrossRef]
24. Rajoria, C.S.; Kumar, R.; Sharma, A.; Singh, D.; Suhag, S. Development of Flat-Plate Building Integrated Photovoltaic/Thermal (BIPV/T) System: A Review. *Mater. Today Proc.* **2020**, *46*, 5342–5352. [CrossRef]
25. Fudholi, A.; Sopian, K. A Review of Solar Air Flat Plate Collector for Drying Application. *Renew. Sustain. Energy Rev.* **2019**, *102*, 333–345. [CrossRef]
26. Pirasteh, G.; Saidur, R.; Rahman, S.M.A.; Rahim, N.A. A Review on Development of Solar Drying Applications. *Renew. Sustain. Energy Rev.* **2014**, *31*, 133–148. [CrossRef]
27. Singh, P.; Shrivastava, V.; Kumar, A. Recent Developments in Greenhouse Solar Drying: A Review. *Renew. Sustain. Energy Rev.* **2018**, *82*, 3250–3262. [CrossRef]
28. Srinivasan, G.; Rabha, D.K.; Muthukumar, P. A Review on Solar Dryers Integrated with Thermal Energy Storage Units for Drying Agricultural and Food Products. *Sol. Energy* **2021**, *229*, 22–38. [CrossRef]
29. Mhd Safri, N.A.; Zainuddin, Z.; Mohd Azmi, M.S.; Zulkifle, I.; Fudholi, A.; Ruslan, M.H.; Sopian, K. Current Status of Solar-Assisted Greenhouse Drying Systems for Drying Industry (Food Materials and Agricultural Crops). *Trends Food Sci. Technol.* **2021**, *114*, 633–657. [CrossRef]
30. Mohana, Y.; Mohanapriya, R.; Anukiruthika, T.; Yoha, K.S.; Moses, J.A.; Anandharamakrishnan, C. Solar Dryers for Food Applications: Concepts, Designs, and Recent Advances. *Sol. Energy* **2020**, *208*, 321–344. [CrossRef]
31. Sivaram, P.M.; Mande, A.B.; Premalatha, M.; Arunagiri, A. Investigation on a Building-Integrated Passive Solar Energy Technology for Air Ventilation, Clean Water and Power. *Energy Convers. Manag.* **2020**, *211*, 112739. [CrossRef]
32. Kumar Verma, S.; Kumar, R.; Barthwal, M.; Rakshit, D. A Review on Futuristic Aspects of Hybrid Photo-Voltaic Thermal Systems (PV/T) in Solar Energy Utilization: Engineering and Technological Approaches. *Sustain. Energy Technol. Assess.* **2022**, *53*, 102463. [CrossRef]

33. Brahim, T.; Jemni, A. Economical Assessment and Applications of Photovoltaic/Thermal Hybrid Solar Technology: A Review. *Sol. Energy* **2017**, *153*, 540–561. [CrossRef]
34. Kulkarni, K.; Afzal, A.; Kim, K.Y. Multi-Objective Optimization of Solar Air Heater with Obstacles on Absorber Plate. *Sol. Energy* **2015**, *114*, 364–377. [CrossRef]
35. Handoyo, E.A.; Ichsani, D.; Prabowo; Sutardi. Numerical Studies on the Effect of Delta-Shaped Obstacles' Spacing on the Heat Transfer and Pressure Drop in v-Corrugated Channel of Solar Air Heater. *Sol. Energy* **2016**, *131*, 47–60. [CrossRef]
36. *ISO 9806*; Solar Energy—Solar Thermal Collectors—Test Methods. ISO: Geneva, Switzerland, 2017; p. 130.
37. Pang, W.; Duck, B.C.; Fell, C.J.; Wilson, G.J.; Zhao, W.; Yan, H. Influence of Multiple Factors on Performance of Photovoltaic-Thermal Modules. *Sol. Energy* **2021**, *214*, 642–654. [CrossRef]
38. Sellami, R.; Amirat, M.; Mahrane, A.; Slimani, M.E.A.; Arbane, A.; Chekrouni, R. Experimental and Numerical Study of a PV/Thermal Collector Equipped with a PV-Assisted Air Circulation System: Configuration Suitable for Building Integration. *Energy Build.* **2019**, *190*, 216–234. [CrossRef]
39. Huang, M.; Wang, Y.; Li, M.; Keovisar, V.; Li, X.; Kong, D.; Yu, Q. Comparative Study on Energy and Exergy Properties of Solar Photovoltaic/Thermal Air Collector Based on Amorphous Silicon Cells. *Appl. Therm. Eng.* **2021**, *185*, 116376. [CrossRef]
40. Rounis, E.D.; Athienitis, A.K.; Stathopoulos, T. BIPV/T Curtain Wall Systems: Design, Development and Testing. *J. Build. Eng.* **2021**, *42*, 103019. [CrossRef]
41. Kim, J.; Park, S.; Kim, J. Experimental Performance of a Photovoltaic-Thermal Air Collector. *Energy Procedia* **2014**, *48*, 888–894. [CrossRef]
42. Guarracino, I.; Freeman, J.; Ramos, A.; Kalogirou, S.A.; Ekins-Daukes, N.J.; Markides, C.N. Systematic Testing of Hybrid PV-Thermal (PVT) Solar Collectors in Steady-State and Dynamic Outdoor Conditions. *Appl. Energy* **2019**, *240*, 1014–1030. [CrossRef]
43. Simón-Allué, R.; Guedea, I.; Coca-Ortegón, A.; Villén, R.; Brun, G. Performance Evaluation of PVT Panel with Phase Change Material: Experimental Study in Lab Testing and Field Measurement. *Sol. Energy* **2022**, *241*, 738–751. [CrossRef]
44. Bambrook, S.M.; Sproul, A.B. Maximising the Energy Output of a PVT Air System. *Sol. Energy* **2012**, *86*, 1857–1871. [CrossRef]
45. Pang, W.; Cui, Y.; Zhang, Q.; Wilson, G.J.; Yan, H. A Comparative Analysis on Performances of Flat Plate Photovoltaic/Thermal Collectors in View of Operating Media, Structural Designs, and Climate Conditions. *Renew. Sustain. Energy Rev.* **2020**, *119*, 109599. [CrossRef]
46. Yu, G.; Yang, H.; Yan, Z.; Kyeredey Ansah, M. A Review of Designs and Performance of Façade-Based Building Integrated Photovoltaic-Thermal (BIPVT) Systems. *Appl. Therm. Eng.* **2020**, *182*, 116081. [CrossRef]
47. Chandrasekar, M.; Senthilkumar, T. Five Decades of Evolution of Solar Photovoltaic Thermal (PVT) Technology—A Critical Insight on Review Articles. *J. Clean. Prod.* **2021**, *322*, 128997. [CrossRef]
48. Kazem, H.A.; Chaichan, M.T.; Al-Waeli, A.H.A.; Sopian, K. Comparison and Evaluation of Solar Photovoltaic Thermal System with Hybrid Collector: An Experimental Study. *Therm. Sci. Eng. Prog.* **2021**, *22*, 100845. [CrossRef]
49. Hussain, F.; Othman, M.Y.H.; Sopian, K.; Yatim, B.; Ruslan, H.; Othman, H. Design Development and Performance Evaluation of Photovoltaic/Thermal (PV/T) Air Base Solar Collector. *Renew. Sustain. Energy Rev.* **2013**, *25*, 431–441. [CrossRef]

Disclaimer/Publisher's Note: The statements, opinions and data contained in all publications are solely those of the individual author(s) and contributor(s) and not of MDPI and/or the editor(s). MDPI and/or the editor(s) disclaim responsibility for any injury to people or property resulting from any ideas, methods, instructions or products referred to in the content.